

# The Phosphatase-Resistant Isoform of CaMKI, Ca<sup>2+</sup>/Calmodulin-Dependent Protein Kinase I $\delta$ (CaMKI $\delta$ ), Remains in Its “Primed” Form without Ca<sup>2+</sup> Stimulation

Yukako Senga,<sup>†,‡</sup> Atsuhiko Ishida,<sup>\*,§</sup> Yasushi Shigeri,<sup>||</sup> Isamu Kameshita,<sup>†</sup> and Noriyuki Sueyoshi<sup>\*,†</sup>

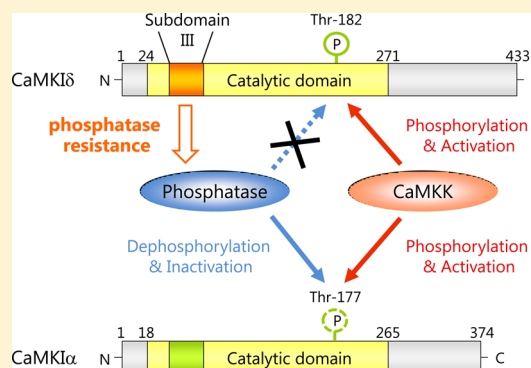
<sup>†</sup>Department of Life Sciences, Faculty of Agriculture, Kagawa University, Miki-cho, Kagawa 761-0795, Japan

<sup>‡</sup>National Institute of Advanced Industrial Science and Technology, Amagasaki, Hyogo 661-0974, Japan

<sup>§</sup>Laboratory of Molecular Brain Science, Graduate School of Integrated Arts and Sciences, Hiroshima University, Higashi-Hiroshima 739-8521, Japan

<sup>||</sup>National Institute of Advanced Industrial Science and Technology, Ikeda, Osaka 563-8577, Japan

**ABSTRACT:** Ca<sup>2+</sup>/calmodulin-dependent protein kinase I (CaMKI) is known to play pivotal roles in Ca<sup>2+</sup> signaling pathways. Four isoforms of CaMKI ( $\alpha$ ,  $\beta$ ,  $\gamma$ , and  $\delta$ ) have been reported so far. CaMKI is activated through phosphorylation by the upstream kinase, CaMK kinase (CaMKK), and phosphorylates downstream targets. When CaMKI was transiently expressed in 293T cells, CaMKI $\alpha$  was not phosphorylated at all under low-Ca<sup>2+</sup> conditions in the cells. In contrast, we found that CaMKI $\delta$  was significantly phosphorylated and activated to phosphorylate cAMP response element-binding protein (CREB) under the same conditions. Herein, we report that the sustained activation of CaMKI $\delta$  is ascribed to its phosphatase resistance resulting from the structure of its N-terminal region. First, we examined whether CaMKI $\delta$  is more readily phosphorylated by CaMKK than CaMKI $\alpha$ , but no significant difference was observed. Next, to compare the phosphatase resistance between CaMKI $\alpha$  and CaMKI $\delta$ , we assessed the dephosphorylation of the phosphorylated CaMKIs by CaMK phosphatase (CaMKP/PPM1F). Surprisingly, CaMKI $\delta$  was hardly dephosphorylated by CaMKP, whereas CaMKI $\alpha$  was significantly dephosphorylated under the same conditions. To date, there have been no detailed reports concerning dephosphorylation of CaMKI. Through extensive analysis of CaMKP-catalyzed dephosphorylation of various chimeric and point mutants of CaMKI $\delta$  and CaMKI $\alpha$ , we identified the amino acid residues responsible for the phosphatase resistance of CaMKI $\delta$  (Pro-57, Lys-62, Ser-66, Ile-68, and Arg-76). These results also indicate that the phosphatase resistance of CaMKI is largely affected by only several amino acids in its N-terminal region. The phosphatase-resistant CaMKI isoform may play a physiological role under low-Ca<sup>2+</sup> conditions in the cells.



Protein kinases regulate a wide variety of cellular processes such as cell proliferation, development, differentiation, and apoptosis.<sup>1</sup> Protein kinases not only phosphorylate their substrate proteins but also undergo autophosphorylation or are phosphorylated by other protein kinases. In many cases, the phosphorylation reactions of protein kinases are important steps in kinase regulation.<sup>2</sup> Consequently, protein phosphatases that dephosphorylate protein kinases are also responsible for the regulation of protein kinases.<sup>3</sup> Thus, intracellular signal transduction is constructed on the basis of the subtle balance between phosphorylation and dephosphorylation.

Multifunctional Ca<sup>2+</sup>/calmodulin-dependent protein kinases (CaMKs), including CaMKI, CaMKII, and CaMKIV, are Ser/Thr protein kinases that are abundantly expressed in the central nervous system. They are thought to act as central downstream effectors of the calcium signal by phosphorylating a variety of neuronal substrates.<sup>4</sup> CaMKII is regulated by Ca<sup>2+</sup>/CaM-dependent autophosphorylation,<sup>5</sup> while CaMKI and CaMKIV are activated by phosphorylation of the Thr residue in the

activation loop by the upstream kinase, CaMKK. CaMKI has been shown to comprise a family of four isoforms ( $\alpha$ ,  $\beta$ ,  $\gamma$ , and  $\delta$ ) encoded by separate genes. CaMKI requires Ca<sup>2+</sup>/CaM and CaMKK, an upstream CaMK that is also activated by Ca<sup>2+</sup>/CaM, for its full activation.<sup>6–8</sup> In previous studies, to investigate the biological significance of CaMKI $\delta$  during zebrafish embryogenesis, we have isolated cDNA clones of CaMKI $\delta$  isoforms (CaMKI $\delta$ -S, CaMKI $\delta$ -L, and CaMKI $\delta$ -LL).<sup>9,10</sup> Knockdown of CaMKI $\delta$ -S/L by morpholino-based antisense oligonucleotides resulted in an increase in the number of abnormal embryos with a short trunk, kinked tail, and small head. In contrast, knockdown of CaMKI $\delta$ -LL resulted in an increase in the number of abnormal embryos with small fins and underdeveloped cartilage. These phenotypes were rescued by co-injection with recombinant CaMKI $\delta$ , but not with their

**Received:** September 26, 2014

**Revised:** May 21, 2015

**Published:** May 21, 2015



kinase-dead mutants. These results suggest that the kinase activity of CaMKI $\delta$  isoforms plays a crucial role in the early stages of the embryogenesis of zebrafish. To date, much about the mechanisms of positive regulation of CaMKs by (auto)-phosphorylation has been published. There is also an increasing amount of evidence of mechanisms of negative regulation of CaMKII and CaMKIV by protein phosphatases.<sup>11–16</sup> However, less attention has been paid to the negative regulation of CaMKI.<sup>17–19</sup>

CaMKI regulates extracellular signal-regulated kinase (ERK)-dependent long-term potentiation,<sup>20</sup> recruitment of calcium-permeable  $\alpha$ -amino-3-hydroxy-5-methyl-4-isoxazole propionic acid (AMPA) receptors,<sup>21</sup> dendritic arborization,<sup>22</sup> neurite outgrowth,<sup>23</sup> filopodia motility, and axon formation.<sup>24,25</sup> It is thought that these phenomena are subtly modulated by dephosphorylation of CaMKI as well as its phosphorylation, like other CaMKs. However, little is known about the mechanisms of CaMKI dephosphorylation. To address this question, we focused on the cellular dephosphorylation of CaMKI in this study.

In a previous study, CaMKI was shown to be activated by phosphorylation by the upstream kinase, CaMKK, in response to stimuli that trigger intracellular Ca<sup>2+</sup> influx.<sup>26</sup> When CaMKI was transiently expressed in 293T cells, CaMKI $\alpha$  was not phosphorylated at all under low-Ca<sup>2+</sup> conditions in the cells. In contrast, CaMKI $\delta$  was significantly phosphorylated and activated to phosphorylate cyclic AMP-responsive element-binding protein (CREB) under the same conditions. These data suggest that CaMKI $\delta$  has unique mechanisms for regulating its kinase activity. We speculated that CaMKK phosphorylates CaMKI $\delta$  as well as CaMKI $\alpha$ , but CaMKI $\delta$  can remain in the phosphorylated form (the potentially active, primed form) because of its phosphatase resistance, even in the absence of Ca<sup>2+</sup> stimulation. In this study, to compare phosphatase resistance between CaMKI $\alpha$  and CaMKI $\delta$ , we explored the mechanism of CaMKI $\delta$  dephosphorylation by CaMK phosphatase (CaMKP/PPM1F),<sup>18,27</sup> which dephosphorylates and regulates multifunctional CaMKs.

## MATERIALS AND METHODS

**Materials.** ATP, bovine serum albumin, anti-CREB antibody, anti-phospho-CREB (pSer133) antibody, and anti- $\beta$ -actin antibody were purchased from Sigma-Aldrich Chemicals. Anti-myc antibody was purchased from Invitrogen. Horseradish peroxidase-conjugated goat anti-mouse IgG and goat anti-rabbit IgG antibodies were obtained from ICN Pharmaceuticals. An anti-His<sub>6</sub> antibody and Silver Stain II Kit were purchased from Wako. Anti-CaMKI $\alpha$  antibody was obtained from Abcam, and anti-CaMKI $\delta$  antibody was obtained from Funakoshi. Recombinant rat CaM<sup>28</sup> and mouse CaMKK $\alpha$ <sup>29</sup> were expressed in *Escherichia coli* and purified as described previously. Antibody against phospho-CaMKI (Thr177) was produced by immunizing BALB/c mice with an antigenic phosphopeptide.<sup>30</sup> Multi-PK antibody (M8C) was prepared as described previously.<sup>31</sup>

**Construction of Plasmids.** pETzCaMKI $\delta$ -LL(WT), pETrCaMKI $\alpha$ (WT), pETrCREB, and pETzCaMKP were prepared as described previously.<sup>10,32–34</sup> pETzCaMKI $\delta$ (1–327) was generated using primers (5'-AGT AGT ATG GGA AGC AGC ATG GAT C-3' and 5'-GCC CAA CTG CAG TCT CCT CAT G-3') and pETzCaMKI $\delta$ (WT). pETrCaMKI $\alpha$ (1–322) was generated using primers (5'-ACC AGC CAG GAG GGA CAG GG-3' and 5'-GCC CAG CTG CAG CTT CCT CA-3') and pETrCaMKI $\alpha$ (WT).

Plasmids for hPPM1A, hPPM1B, and hPPM1D were generated using sense primers (5'-TTT TCT AGA ATG GGA GCA TTT TTA GAC AAG CCA-3' for hPPM1A, 5'-TTT TCT AGA ATG GGT GCA TTT TTG GAT AAA CCC-3' for hPPM1B, and 5'-TTT GCT AGC ATG GCG GGG CTG GTA CTC GC-3' for hPPM1D), antisense primers (5'-AAA CTC GAG CCA CAT ATC ATC TGT TGA TGT AGA GTC AG-3' for hPPM1A, 5'-AAA CTC GAG TAT TTT TTC ACC ACT CAT CTT TGT CCC-3' for hPPM1B, and 5'-AAA GTC GAC ATA GCA AAC ACA AAC AGT TTT CCT GTG-3' for hPPM1D), and KIBB5611, KIBB8150, and KIEE4537 (Kazusa DNA Research Institute) as a template, respectively. The XbaI (underlined)–XhoI (bold underline) or NheI (italic underline)–SalI (bold and italic underline) fragments were inserted into the XbaI–XhoI or NheI–SalI sites of pET-23a(+), respectively (Novagen).

Plasmids for rCaMKI $\alpha$ /zCaMKI $\delta$  chimera mutants were constructed by the inverse polymerase chain reaction (PCR) method<sup>35</sup> with sense primers (5'-CCT AAA AAA GCT CTG AAG GGG AAG-3' for chimera 1, 5'-ACT ATG GGC ATC GTC CAT CGA G-3' for chimera 2, 5'-GCT CAG AAA CCG TAC AGT AAA GCT GT-3' for chimera 3, 5'-GAG AAC ATA GTG GCT CTT GAA GAC ATC T-3' for chimera 1-1, 5'-ATG CAG CTT GTG TCT GGA GGA GA-3' for chimera 1-2, and 5'-AAA GAC GCC AGC ACA CTC ATC AG-3' for chimera 1-3), antisense primers (5'-AAT GCA TTT GAT GGC CAC CAG T-3' for chimera 1, 5'-GTG CAG GTA CTT GAC AGC ATC CAG-3' for chimera 2, 5'-CAG GAC CTC AGG GGC CAC AT-3' for chimera 3, 5'-GTG CTT GAT CTT GTG TAA GAC GGC-3' for chimera 1-1, 5'-GAT GAG GTA GAG GTG GCC CCC-3' for chimera 1-2, and 5'-TTC TGT GTA GAA TCC TTT CTC CAC AAT T-3' for chimera 1-3), and pETrCaMKI $\alpha$ (WT)/zCaMKI $\delta$ (WT) as a template. The 5'-ends of the PCR fragments were then phosphorylated by T4 polynucleotide kinase (Nippon Gene) and self-ligated by T4 DNA ligase (Nippon Gene). The various zCaMKI $\delta$  and rCaMKI $\alpha$  mutants containing an NheI site at the 5'-ends and an XhoI site at the 3'-ends were inserted into the pET-23a(+) vector (Novagen).

Mutagenesis of Pro-57, Lys-62, Ser-66, Ile-68, and Arg-76 was performed by the inverse PCR method with sense primers (5'-GCT AAA AAA GCT CTG AAG GGG AAG-3' for P57A, 5'-GAG GGG AAG GAG AGC AGC ATC G-3' for K62E, 5'-GGC AGC ATC GAG AAC GAG ATC G-3' for S66G, 5'-AGC AGC ATG GAG AAC GAG ATC G-3' for I68M, and 5'-CAC AAA ATT AAG CAT GAG AAC ATA GTG-3' for R76H; underlines show the mutation sites), antisense primers (5'-GAT GCA TTT CAC AGC GTA CAT CTT T-3' for P57A, 5'-CAG AGC TTT TTT AGG GAT GCA TTT CA-3' for K62E, 5'-CTC CTT CCC CTT CAG AGC TTT TTT-3' for S66G and I68M, and 5'-CAG AAC GGC GAT CTC GTT CTC G-3' for R76H), and pETzCaMKI $\delta$ (WT) as a template. The 5'-ends of the PCR fragments were then phosphorylated by T4 polynucleotide kinase and self-ligated by T4 DNA ligase. The various zCaMKI $\delta$  and rCaMKI $\alpha$  mutants containing an NheI site at the 5'-ends and XhoI site on the 3'-ends were inserted into the pET-23a(+) vector.

For mammalian cells, the following plasmids were prepared. pczCaMKI $\delta$ , pcrCaMKI $\alpha$ , pcmCaMKI $\delta$ , and pczCaMKP were prepared as described previously.<sup>10,30,32</sup> pcrCREB was generated by PCR using specific primers (5'-GCT AGC GTT ATG ACC ATG GAC TCT GGA GC-3' and 5'-CTC GAG ATC TGA CTT GTG GCA GTA AAG G-3') and

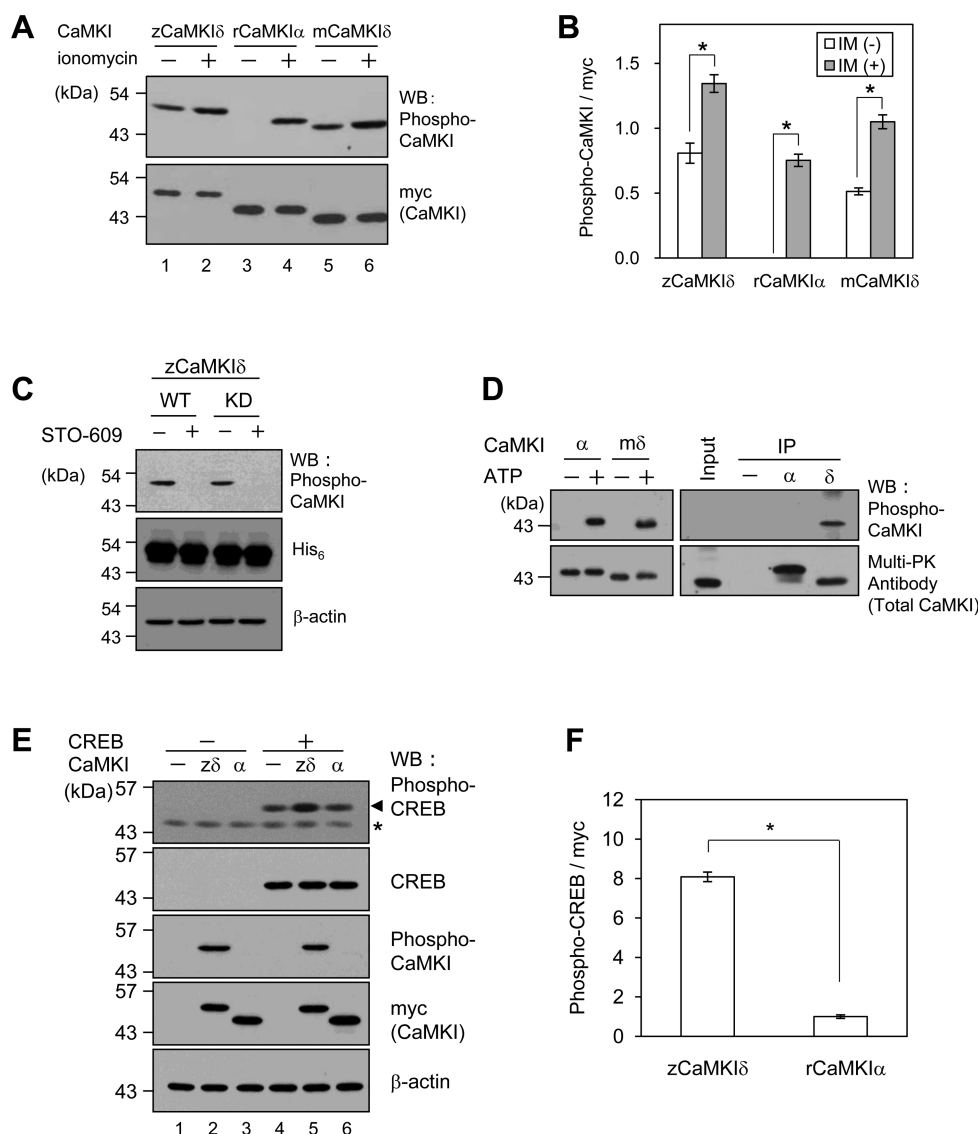


**Figure 1.** Phosphorylation and activation of CaMKI in mammalian cells. (A) pcDNA-CaMKIs were transfected into 293T cells. Cells expressing the indicated myc-tagged proteins were stimulated with 1  $\mu$ M ionomycin for 5 min and lysed with SDS sample buffer. The cell lysates (20  $\mu$ g of protein) were subjected to SDS-PAGE and then analyzed by Western blotting with an anti-phospho-CaMKI antibody (top panel). The lysates were also analyzed by Western blotting using anti-myc antibodies to detect myc-tagged CaMKI (bottom panel). (B) The Western blot using the phospho-CaMKI antibody was quantified by Scion Image software. Data are shown as means  $\pm$  SD of three independent experiments. (C) pcDNA-CaMKI $\delta$ (WT) or the kinase-dead (KD) mutant was transfected into 293T cells and then cultured for 20 h either with (+) or without (–) 10  $\mu$ g/mL STO-609. Cells expressing the indicated myc-tagged proteins without prior stimulation were lysed with SDS sample buffer. The cell lysates were subjected to SDS-PAGE and then analyzed by Western blotting with anti-phospho-CaMKI, anti-His<sub>6</sub> (for CaMKI detection), and anti- $\beta$ -actin antibodies. (D) Purified His<sub>6</sub>-tagged CaMKI $\alpha$  and CaMKI $\delta$  (20 ng) were phosphorylated by CaMKK. They were subjected to 10% SDS-PAGE and detected by Western blotting with anti-phospho-CaMKI and M8C Multi-PK antibodies (left panel). Endogenous CaMKI $\alpha$  or CaMKI $\delta$  proteins were immunoprecipitated from 293T cell lysates with anti-CaMKI $\alpha$  or anti-CaMKI $\delta$  antibodies and detected by Western blotting using anti-phospho-CaMKI and M8C antibodies (right panel). (E) pcDNA-CaMKIs were cotransfected with pcDNA-rCREB into 293T cells. Cells expressing the indicated myc-tagged proteins without prior stimulation were lysed with SDS sample buffer. The cell lysates (20  $\mu$ g of protein) were subjected to SDS-PAGE and then analyzed by Western blotting with anti-phospho-CREB(Ser133), anti-CREB, anti-phospho-CaMKI, anti-myc (for CaMKI detection), and anti- $\beta$ -actin antibodies. The arrowhead and the asterisk indicate the phospho-CREB and the nonspecific band, respectively. (F) CREB phosphorylation mediated by the transfected CaMKIs shown in panel E was quantified by Scion Image software. The band intensity of the background phosphorylation (lane 4) was subtracted from that of the zCaMKI $\delta$ -induced phosphorylation (lane 5) or rCaMKI $\alpha$ -induced phosphorylation (lane 6) to yield quantitation of phosphorylation due to the transfected CaMKIs. The values obtained were normalized to the respective CaMKI protein detected by Western blotting with an anti-myc antibody. Data are shown as means  $\pm$  SD of three independent experiments. The asterisks denote significant differences as determined by a Student's *t* test ( $p < 0.005$ ).

pETrCREB<sup>34</sup> as a template. pczCaMKI $\delta$  (P57A, K62E, S66G, I68M, R76H) was generated by PCR using specific primers (5'-AAA AAG CTT GTT ATG GCT CGG GAG AAC GGA GA-3' and 5'-TTT CTC GAG CGC TTG GTC CCA GTT ACC ACT GTG C-3') and pETzCaMKI $\delta$  (P57A, K62E, S66G,

I68M, R76H) as a template. The HindIII (underline)-XhoI (bold underline) fragment was inserted into the HindIII-XhoI sites of pcDNA3.1(+)/myc-His B (Invitrogen).

**Cell Culture and Transfection.** 293T cells were cultured in Dulbecco's modified Eagle's medium (DMEM) (Wako)



containing 10% heat-inactivated fetal calf serum (FCS). Cells were grown at 37 °C in a humidified incubator with a 5% CO<sub>2</sub>/95% air atmosphere. Transfections of 293T cells were performed using Lipofectamine 2000 (Invitrogen) according to the manufacturer's instructions. 293T cells ( $6 \times 10^5$ ) were plated in a 35 mm dish in 2 mL of DMEM containing 10% FCS. After being cultured for 24 h, the cells were incubated for 24 h in 1 mL of DMEM containing 5% FCS, 6  $\mu$ L of Lipofectamine 2000, and 3  $\mu$ g of plasmid DNA for transfection. Transfected cells were starved in serum-free DMEM for 6 h and then stimulated by addition of 1  $\mu$ M ionomycin at 37 °C. After stimulation, the medium was removed and 150  $\mu$ L of sodium dodecyl sulfate (SDS) sample buffer was added to stop the reaction. The samples were boiled for 5 min, electrophoresed on a SDS–polyacrylamide gel, and analyzed by Western blotting.

**Immunoprecipitation.** 293T cells were lysed in an immunoprecipitation buffer [20 mM Tris-HCl (pH 7.5), 150 mM NaCl, 1 mM EDTA, 0.5% Triton X-100, 1 mM sodium orthovanadate, 1 mM phenylmethanesulfonyl fluoride, 1 mM dithiothreitol (DTT), 10  $\mu$ g/mL chymostatin, 10  $\mu$ g/mL pepstatin, 10  $\mu$ g/mL leupeptin, and 10  $\mu$ g/mL antipain]. The supernatant was incubated with an anti-CaMKI $\alpha$  antibody or anti-CaMKI $\delta$  antibody coupled to protein G-Sepharose at 4 °C for 2 h in the immunoprecipitation buffer. After being washed with the immunoprecipitation buffer to remove unbound proteins, the Sepharose gel was boiled with 2 $\times$  SDS–polyacrylamide gel electrophoresis (PAGE) sample buffer. The resulting supernatant was subjected to SDS–PAGE and analyzed by Western blotting with the indicated antibodies.

**Expression and Purification of Recombinant Proteins.** pETCaMKIs, pETCREB, and pETCaMK phosphatases were introduced into *E. coli* strain BL21(DE3). For recombinant CaMKIs, the transformed bacteria were grown at 37 °C to an OD<sub>600</sub> of 0.6–0.8, and then isopropyl  $\beta$ -D-thiogalactopyranoside (IPTG) was added to a final concentration of 0.1 mM. After 24 h at 25 °C, the bacteria were harvested by centrifugation (2300g) at 2 °C for 10 min and suspended in buffer A [20 mM Tris-HCl (pH 7.5), 150 mM NaCl, 0.05% Tween 40, and 1 mM phenylmethanesulfonyl fluoride]. For recombinant zCaMKP, hCaMKP, hPPM1A, and hPPM1B, the transformed bacteria were cultured at 25 °C for 24 h without IPTG induction and collected as described above. For recombinant hPPM1D, the transformed bacteria were cultured at 18 °C for 6 h via IPTG induction and collected as described above. After the harvest, the bacterial cells were sonicated and cell debris was removed by centrifugation (20000g) at 4 °C for 10 min, and the obtained supernatant was loaded onto a HiTrap Chelating HP column (GE Healthcare Bio-Sciences) pre-equilibrated with buffer A. The column was washed with buffer A, buffer A containing 20 mM imidazole, or buffer A containing 50 mM imidazole and then eluted with buffer A containing 200 mM imidazole. The purified fractions were pooled, dialyzed against 20 mM Tris-HCl (pH 7.5) containing 0.05% Tween 40 and 1 mM 2-mercaptoethanol, and used for the characterization of the enzyme.

**SDS–PAGE and Western Blotting.** SDS–PAGE was performed essentially according to the method of Laemmli<sup>36</sup> on slab gels consisting of a 10 or 12% acrylamide separation gel and a 3% stacking gel. The resolved proteins were electrophoretically transferred to nitrocellulose membranes (Hybond-ECL, GE Healthcare Bio-Sciences), and immunoreactive

protein bands were detected essentially according to a method described previously.<sup>29</sup>

**Phosphorylation of CaMKI by CaMKK.** Phosphorylation of CaMKI was conducted at 30 °C for the indicated time in a reaction mixture (20  $\mu$ L) consisting of 40 mM Hepes-NaOH (pH 8.0), 5 mM Mg(CH<sub>3</sub>COO)<sub>2</sub>, 2 mM DTT, 0.5 mM CaCl<sub>2</sub>, 1  $\mu$ M CaM, 2.5  $\mu$ g of CaMKI, 125 ng of CaMKK, and 100  $\mu$ M ATP. The reaction was initiated by the addition of CaMKI and stopped by the addition of 20  $\mu$ L of 2 $\times$  SDS–PAGE sample buffer, followed by Western blotting.

**Protein Phosphatase Assay Using Phosphoproteins as Substrates.** The protein phosphatase assay was conducted using CaMKI as a phosphoprotein substrate. Recombinant CaMKI (2.5  $\mu$ g) was phosphorylated by CaMKK (125 ng) at 30 °C for 30 min in a reaction mixture containing 50 mM Hepes-NaOH (pH 7.5), 10 mM Mg(CH<sub>3</sub>COO)<sub>2</sub>, 0.1 mM EGTA, 1  $\mu$ M CaM, 0.5 mM CaCl<sub>2</sub>, and 100  $\mu$ M ATP. The reaction was stopped with termination buffer (80  $\mu$ L) containing ice-cold 50 mM Tris-HCl (pH 7.5), 0.05% Tween 40, 2 mM DTT, and 2.5 mM EGTA. Dephosphorylation of phospho-CaMKI was conducted at 30 °C for 10 min in a reaction mixture containing 50 mM Tris-HCl (pH 8.0), 5 mM MnCl<sub>2</sub>, 0.1 mM EGTA, 0.01% Tween 20, 2 mM DTT, 100 ng of phospho-CaMKI, and 2.5, 5, or 10 ng of CaMKP. The reaction was started by addition of CaMKP and terminated by addition of an equal volume of 2 $\times$  SDS–PAGE sample buffer. The sample was then subjected to SDS–PAGE and analyzed by Western blotting using phospho-CaMKI antibody.

**Other Methods.** Protein concentrations were determined by the method of Bensadoun and Weinstein using bovine serum albumin as a standard.<sup>37</sup> Nucleotide sequences were determined by the dideoxynucleotide chain termination method with BigDye Terminator Cycle Sequencing Ready Reaction Kit version 3.1 (Applied Biosystems) and a DNA sequencer (model 3100, Applied Biosystems).

## RESULTS

**Phosphorylation and Activation of CaMKI $\delta$ .** Our studies of the biochemical properties of CaMKIs revealed that the zebrafish CaMKI $\delta$  isoform was significantly phosphorylated under low-Ca<sup>2+</sup> conditions (resting state) in the cells. In an effort to clarify the molecular mechanisms underlying the anomalous phosphorylation of zCaMKI $\delta$ , we examined the phosphorylation of exogenously expressed zCaMKI $\delta$  in 293T cells, as well as that of mouse CaMKI $\delta$ . Because zCaMKI $\alpha$  had not been examined in detail, we used rat CaMKI $\alpha$ , of which the subcellular localization has been shown to be very similar to that of zCaMKI $\delta$ ,<sup>9</sup> as a control. In living cells, CaMK was activated by stimulation with ionomycin, a calcium ionophore (Figure 1A, lanes 2, 4, and 6, and Figure 1B). When CaMKI isoforms were transiently expressed in 293T cells, CaMKI $\alpha$  was not phosphorylated at all under low-Ca<sup>2+</sup> conditions in the cells (Figure 1A, lane 3, and Figure 1B). In contrast, both zCaMKI $\delta$  and mCaMKI $\delta$  were significantly phosphorylated under the same conditions (Figure 1A, lanes 1 and 5, and Figure 1B), suggesting that the observed sustained phosphorylation was not characteristic of the zebrafish enzyme, but a common property of CaMKI $\delta$  conserved in vertebrates. Next, to confirm that CaMKI $\delta$  is phosphorylated by CaMKK in 293T cells, we examined whether phosphorylation of zCaMKI $\delta$  by endogenous CaMKK is inhibited by the selective CaMKK inhibitor, STO-609. Under low-Ca<sup>2+</sup> conditions in the cells, the level of phosphorylation of zCaMKI $\delta$ (WT) and the kinase-dead

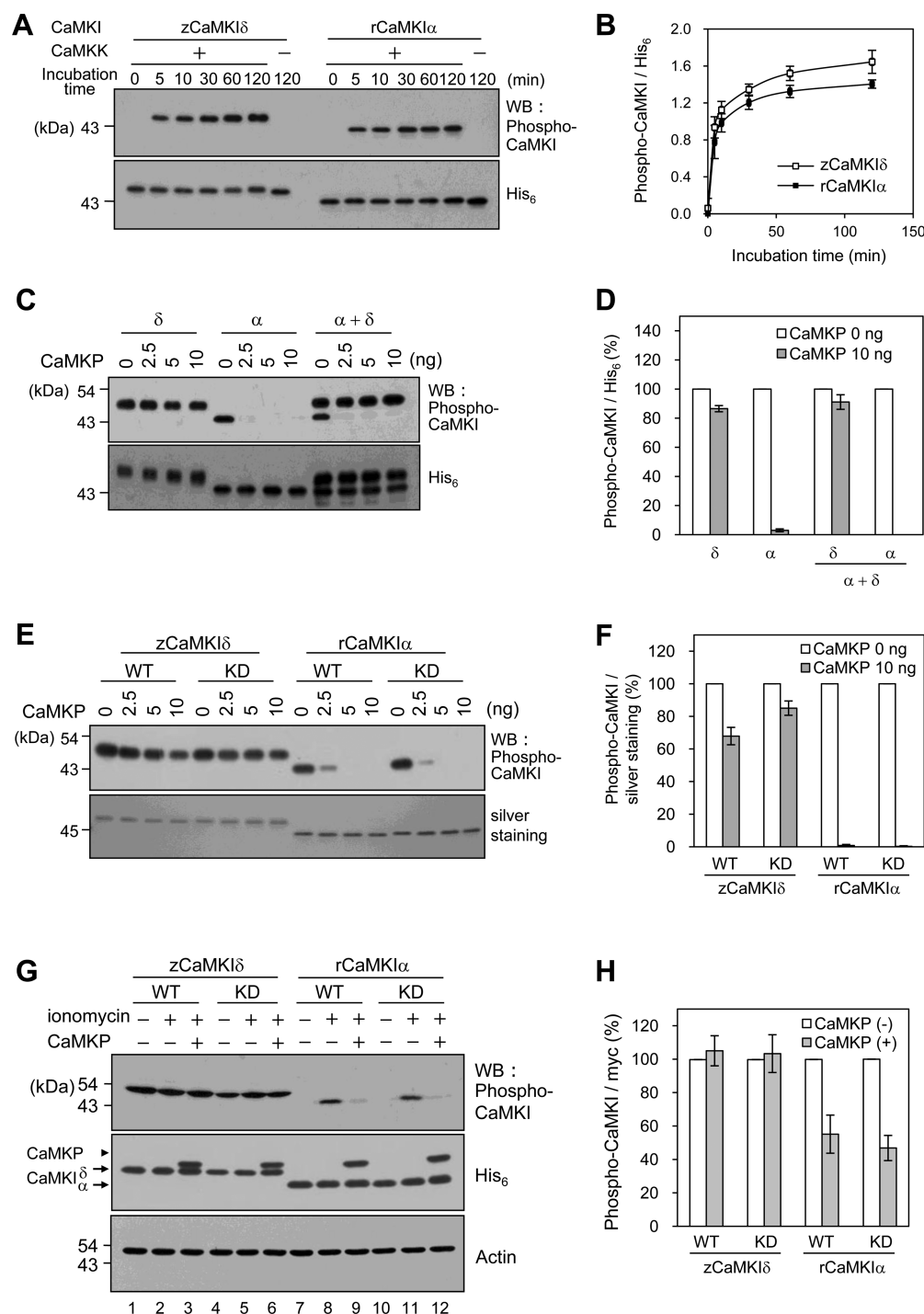


**Figure 2.** Dephosphorylation of CaMKIs by CaMKP *in vitro* and in mammalian cells. (A) Time course of phosphorylation of CaMKIs by mouse CaMKK $\alpha$ . Purified CaMKIs were incubated with Ca $^{2+}$ /CaM in the presence or absence of CaMKK $\alpha$  in a reaction mixture. After incubation at 30 °C, the reactions were stopped by addition of 2 $\times$  SDS–PAGE sample buffer, and the mixtures were subjected to 10% SDS–PAGE and then analyzed by Western blotting with anti-phospho-CaMKI and anti-His $_6$  antibodies (for CaMKI detection). (B) Phospho-CaMKIs (A, top panel) and total CaMKIs (A, bottom panel) were quantified by Scion Image software, and the ratios of phospho-CaMKI to total CaMKI (His $_6$ ) were calculated. Data are means  $\pm$  SD of three independent determinations. (C) The phosphatase activity of CaMKP was determined using phospho-CaMKI as a substrate. Dephosphorylation of CaMKI (CaMKI $\delta$ , CaMKI $\alpha$ , and their combination) was monitored by Western blotting with an anti-phospho-CaMKI antibody (top panel). The total CaMKI level was examined by Western blotting with an anti-His $_6$  antibody (bottom panel). (D) Phospho-CaMKI (C, top panel) and total CaMKI (C, bottom panel) were quantified by Scion Image software, and they are shown as phospho-CaMKI/total CaMKI (His $_6$ ). Data are means  $\pm$  SD of three independent determinations. (E) The phosphatase activity of CaMKP was determined using phospho-CaMKI as a substrate. Dephosphorylation of CaMKI was monitored by Western blotting with an anti-phospho-CaMKI antibody (top panel), and the total CaMKI level was examined by silver staining (bottom panel). (F) Phospho-CaMKI (E, top panel) and total CaMKI (E, bottom panel) were quantified by Scion Image software, and they are shown as phospho-CaMKI/total CaMKI. Data are means  $\pm$  SD of three independent determinations. (G) 293T cells transfected with pcDNA-CaMKIs alone or together with pcDNA-CaMKP were cultured for 24 h. Subsequently, the cells were cultured in serum-free medium for 6 h and stimulated with 1  $\mu$ M ionomycin for 5 min. The cells were lysed with SDS–PAGE sample

Figure 2. continued

buffer and analyzed by Western blotting with anti-phospho-CaMKI antibody (top panel). The lysates were also analyzed by Western blotting using anti-myc antibody to detect myc-tagged CaMKIs (arrows) and myc-tagged CaMKP (arrowhead) (middle panel).  $\beta$ -Actin was also examined for loading control (bottom panel). (H) Quantification of phospho-CaMKI (G, top panel) and CaMKI (G, middle panel, arrows) by Scion Image software is shown as phospho-CaMKI/total CaMKI (myc). Data are means  $\pm$  SD of three independent determinations.

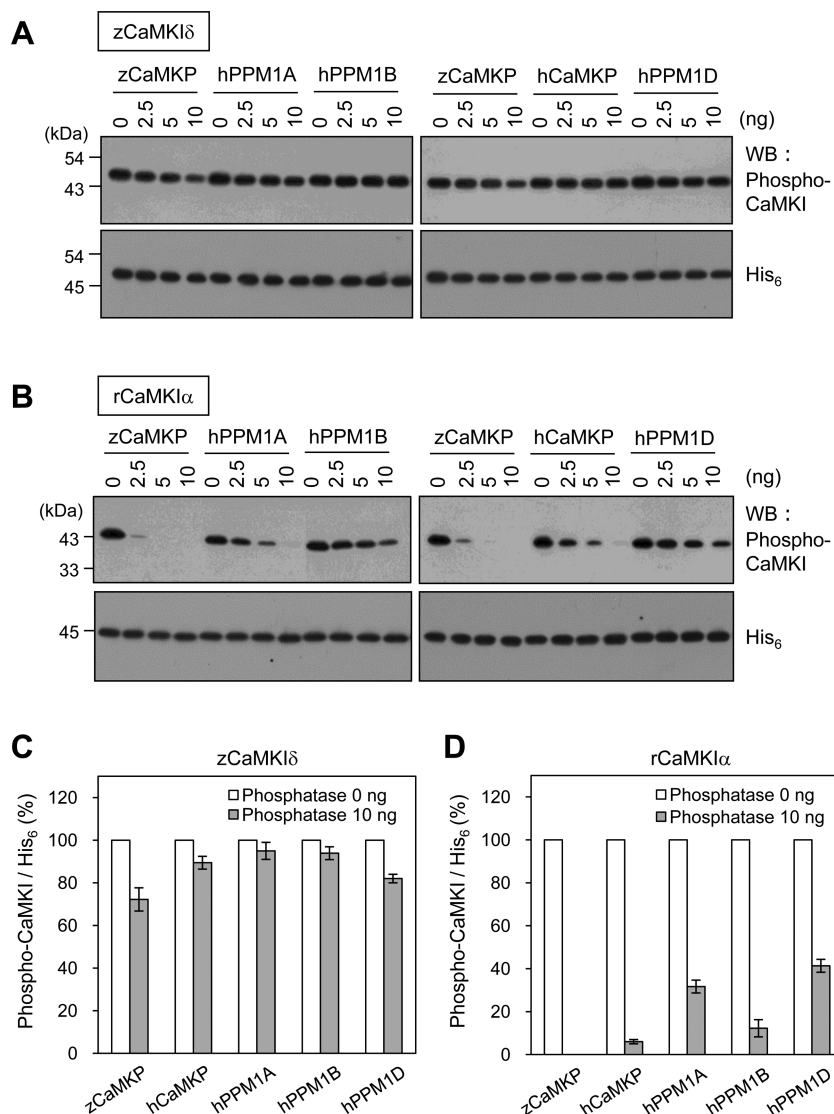


**Figure 3.** Dephosphorylation of CaMKIs by other Ser/Thr phosphatases such as PPM1A, PPM1B, and PPM1D *in vitro*. (A and B) The phosphatase activity was determined using phospho-CaMKI $\delta$  and phospho-CaMKI $\alpha$  as substrates, respectively. Dephosphorylation of CaMKIs was monitored by Western blotting with an anti-phospho-CaMKI antibody (top panel), and the total CaMKI level was examined by Western blotting with an anti-His<sub>6</sub> antibody (bottom panel). (C and D) Phospho-CaMKI (A and B, top panel) and CaMKI (A and B, bottom panel) were quantified by Scion Image software, and they are shown as phospho-CaMKI/total CaMKI (His<sub>6</sub>). Data are means  $\pm$  SD of three independent determinations.

mutant (KD) was significantly reduced after treatment with STO-609 (Figure 1C). Therefore, we used the zebrafish enzyme in the following characterization of CaMKI $\delta$ .

Furthermore, to examine the phosphorylation of endogenous CaMKI, the cell lysates were immunoprecipitated with an anti-CaMKI $\alpha$  or anti-CaMKI $\delta$  antibody (Figure 1D). In this experiment, endogenous CaMKIs were detected by Western blotting with Multi-PK antibody. The Multi-PK antibody was produced to detect a wide variety of Ser/Thr protein kinases<sup>31</sup> and has been used for the detection of various protein kinases. When Multi-PK antibody was used in the Western blotting analysis, similar immunoreactive bands of CaMKI $\alpha$  and

CaMKI $\delta$  were detected with and without ATP. That is, the Multi-PK antibody detected nonphosphorylated CaMKI as well as phosphorylated CaMKI. When the cell lysates were immunoprecipitated with an anti-CaMKI $\delta$  antibody, the CaMKI $\delta$  protein was phosphorylated under low-Ca<sup>2+</sup> conditions in the cells (Figure 1D, right panel). In contrast, CaMKI $\alpha$  was not phosphorylated at all under the same conditions.

Next, to examine whether CaMKI $\delta$  is phosphorylated and activated to phosphorylate CREB under low-Ca<sup>2+</sup> conditions in the cells, we co-expressed CaMKI and CREB in 293T cells. The phosphorylation level of CaMKI and CREB was analyzed by

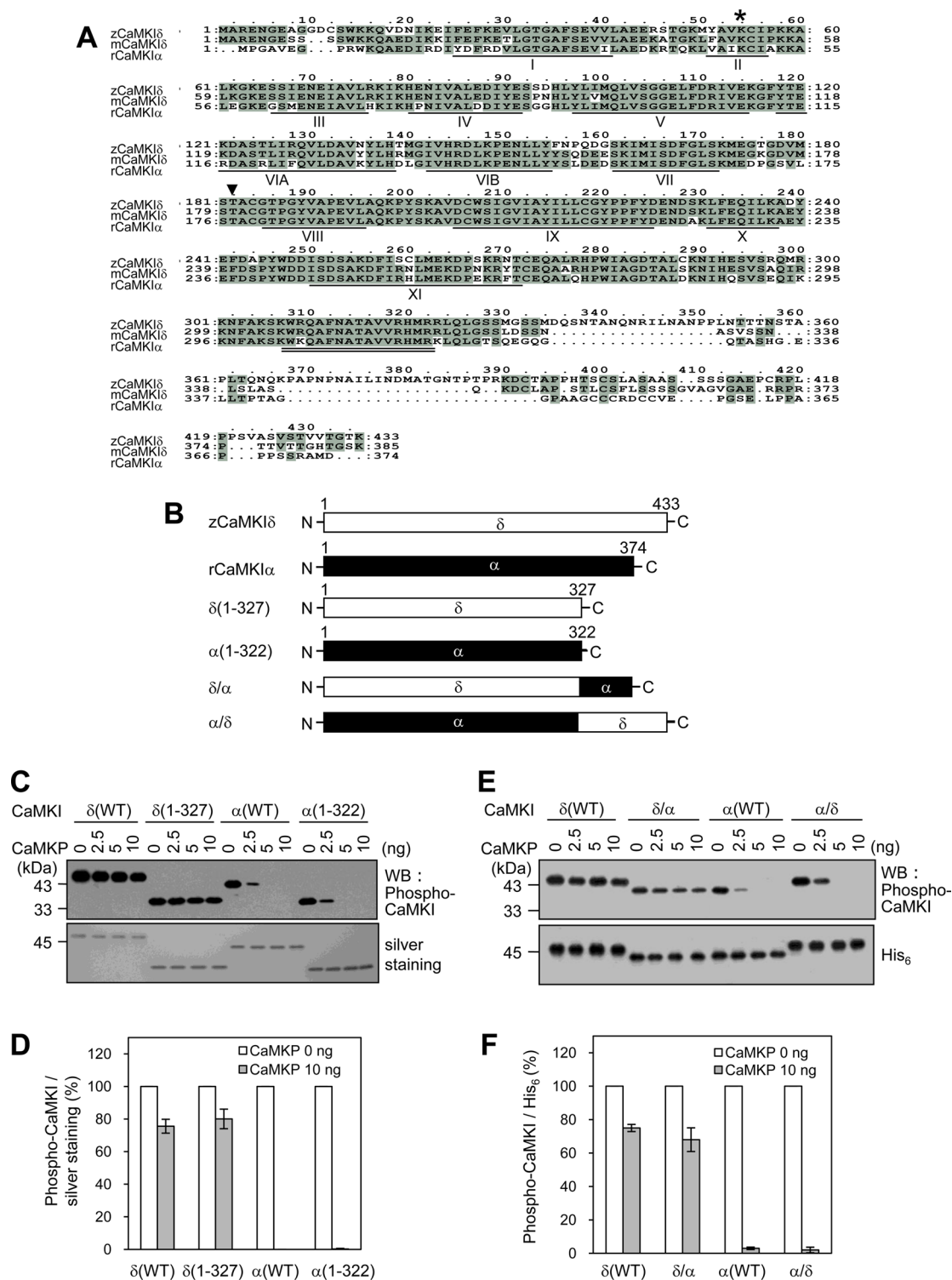


**Figure 4.** Dephosphorylation of CaMKI C-terminal deletion mutants and chimera mutants by CaMKP. (A) Alignment of amino acid sequences of zCaMKI $\delta$  (GenBank accession number BC160632), mCaMKI $\delta$  (GenBank accession number BC141413), and rCaMKI $\alpha$  (GenBank accession number NP598687). The identical amino acids are highlighted in gray. Twelve subdomains specific to protein kinases are shown with solid underlines. The ATP-binding site and the CaMKK phosphorylation site are shown with an asterisk and an arrowhead, respectively. The putative CaM-binding domains are double-underlined. (B) Schematic illustration of the primary structures of zCaMKI $\delta$ (WT), rCaMKI $\alpha$ (WT), zCaMKI $\delta$ (1–327), rCaMKI $\alpha$ (1–322), zCaMKI $\delta$ (323–374) ( $\delta/\alpha$ ), and rCaMKI $\alpha$ (1–322)/zCaMKI $\delta$ (328–433) ( $\alpha/\delta$ ) chimeric mutants. zCaMKI $\delta$  and rCaMKI $\alpha$  are shown by a white box and a black box, respectively. (C and E) The phosphatase activity of CaMKP was determined using the indicated phospho-CaMKI mutant as a substrate. Dephosphorylation of the WT and mutant CaMKI was monitored by Western blotting with an anti-phospho-CaMKI antibody (top panel). The total CaMKI level was examined by silver staining (C, bottom panel) or by Western blotting using anti-His<sub>6</sub> antibody (E, bottom panel). (D and F) Relative phosphorylation levels of CaMKIs were quantified by Scion Image software and indicated as phospho-CaMKI/total CaMKI. Data are means  $\pm$  SD of three independent determinations.



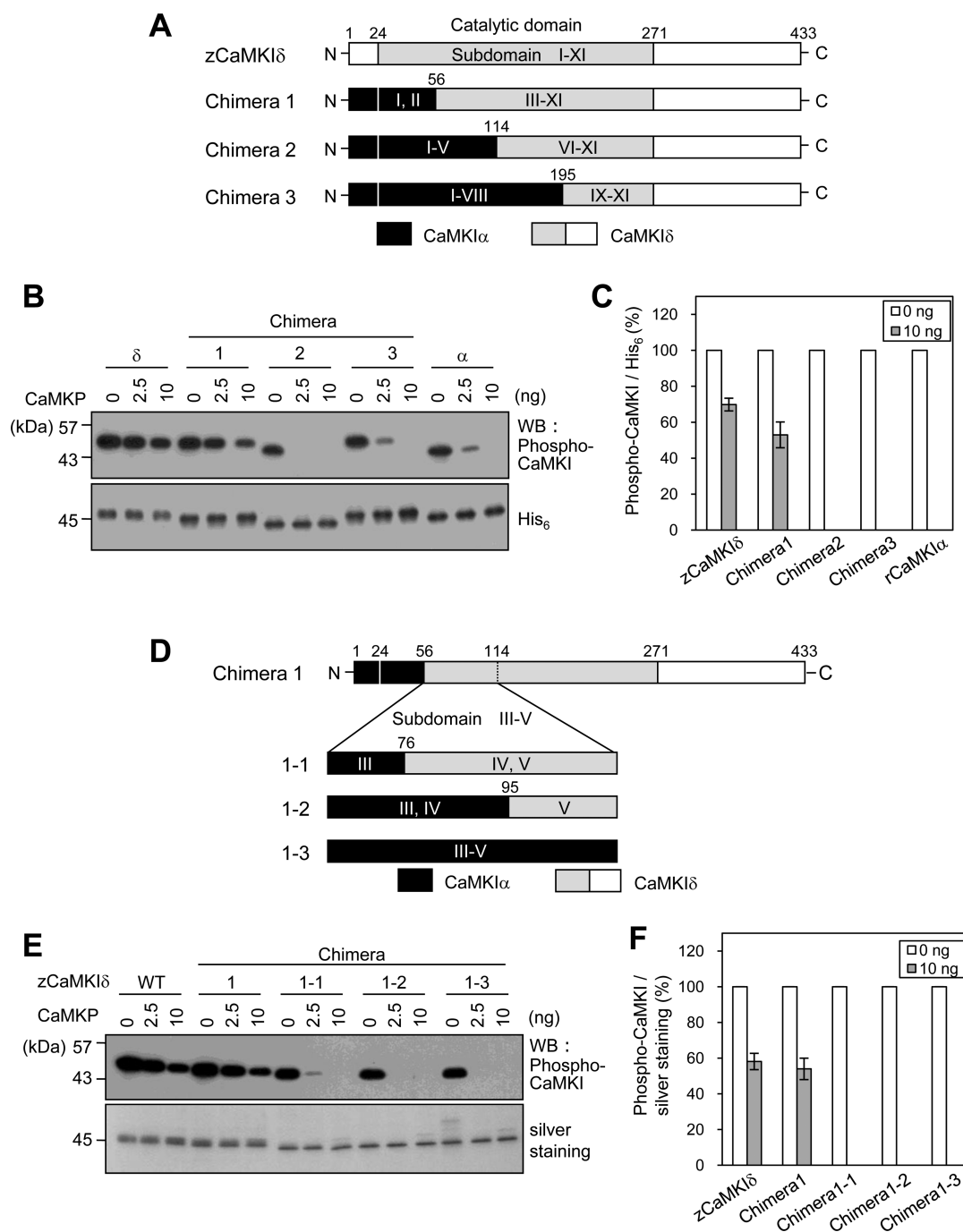


**Figure 5.** Dephosphorylation of zCaMKIδ N-terminal chimera mutants by CaMKP. (A) Schematic illustration of the primary structures of zCaMKIδ and N-terminal chimera mutants. The catalytic domains of zCaMKIδ and rCaMKIα are shown by gray boxes and black boxes, respectively. (B) The phosphatase activity of CaMKP was determined using the indicated phospho-CaMKI chimera as a substrate. Dephosphorylation of the CaMKI chimeras was monitored by Western blotting with an anti-phospho-CaMKI antibody (top panel), and the total CaMKI level was examined by Western blotting using an anti-His<sub>6</sub> antibody (bottom panel). (C) Relative phosphorylation levels of CaMKI chimeras were quantified by Scion Image software and indicated as phospho-CaMKI/total CaMKI. Data are means  $\pm$  SD of three independent determinations. (D) Schematic illustration of the primary structures of the Chimera 1 mutant and the additional N-terminal chimera mutants (chimeras 1-1, 1-2, and 1-3). The catalytic domains of zCaMKIδ and rCaMKIα are shown by gray boxes and black boxes, respectively. (E) The phosphatase activity of CaMKP was determined using the indicated phospho-CaMKI chimeras as a substrate. Dephosphorylation of CaMKI was monitored by Western blotting with an anti-phospho-CaMKI antibody (top panel), and the total CaMKI levels were examined by silver staining (bottom panel). (F) Relative phosphorylation levels of CaMKI chimeras were quantified by Scion Image software and indicated as phospho-CaMKI/total CaMKI. Data are means  $\pm$  SD of three independent determinations.

Western blotting using a phospho-CaMKI-specific antibody and a phospho-CREB-specific antibody. As shown in Figure 1E, CaMKIδ, but not CaMKIα, was significantly phosphorylated and activated to phosphorylate CREB under low-Ca<sup>2+</sup>

conditions in the cells (Figure 1E, lanes 5 and 6, and Figure 1F).

**Dephosphorylation of CaMKI by CaMKP *in Vitro* and *in Vivo*.** The significant phosphorylation and activation of



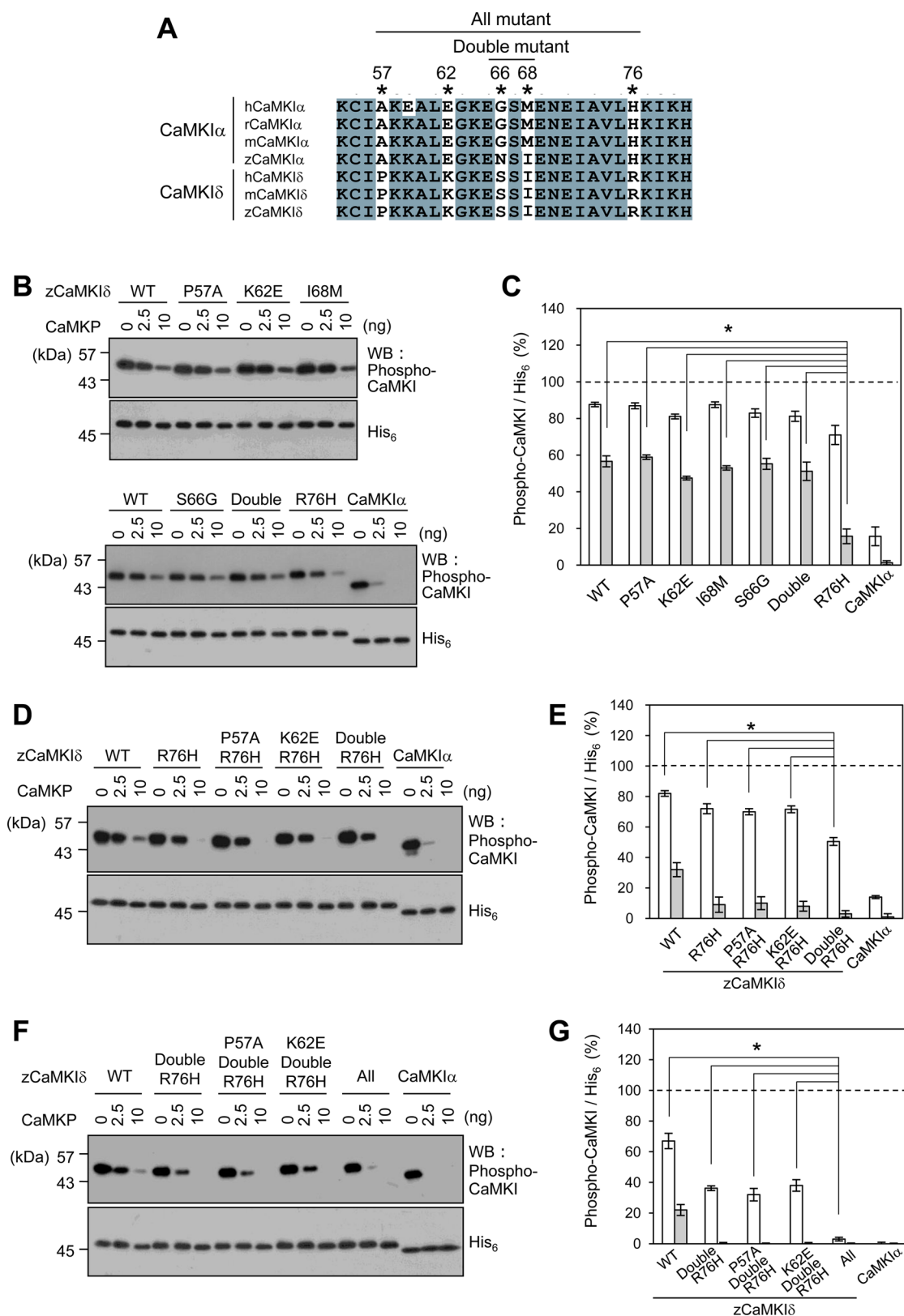


**Figure 6.** Effects of subdomain III of zCaMKI $\delta$ . (A) Comparison of the amino acid sequences of subdomain III of CaMKIs. Asterisks show the different amino acids between CaMKI $\alpha$  and CaMKI $\delta$ . These residues in CaMKI $\delta$  were mutated to those in CaMKI $\alpha$  in the following experiments. (B, D, and F) The phosphatase activity of CaMKP was determined using the indicated mutant of phospho-CaMKI as a substrate. Dephosphorylation of CaMKI was monitored by Western blotting with anti-phospho-CaMKI antibody (top panel), and the total CaMKI was detected by an anti-His<sub>6</sub> antibody (bottom panel). (C, E, and G) Relative phosphorylation levels of CaMKI were quantified by Scion Image software and indicated as phospho-CaMKI/total CaMKI. The values are expressed as a percentage of the control reaction (CaMKP 0 ng, shown as a dotted line). White bars and gray bars show dephosphorylation by 2.5 and 10 ng of CaMKP, respectively. Data are means  $\pm$  SD of three independent determinations. Asterisks denote significant differences as determined by a Student's *t* test ( $p < 0.005$ ).

CaMKI $\delta$  under low-Ca<sup>2+</sup> conditions in the cells may exist because of enhanced phosphorylation by CaMKK. To examine whether CaMKI $\delta$  is more readily phosphorylated by CaMKK than CaMKI $\alpha$ , we prepared recombinant CaM, CaMKK, and CaMKI expressed in *E. coli*. When CaMKIs were phosphorylated by CaMKK in the presence of Ca<sup>2+</sup>/CaM and CaMKK, only a modest difference in phosphorylatability was observed between them (Figure 2A,B). Next, to compare the phosphatase resistance of CaMKI $\alpha$  and CaMKI $\delta$ , we conducted phosphatase assays using CaMKP, which dephosphorylates and regulates multifunctional CaMKs. Surprisingly, CaMKI $\delta$  was highly resistant to dephosphorylation by CaMKP, whereas CaMKI $\alpha$  was significantly dephosphorylated under the same conditions (Figure 2C,D). To examine whether the phosphatase resistance of CaMKI $\delta$  depends on kinase activity, we performed phosphatase assays using kinase-dead (KD) mutants of CaMKI $\delta$  and CaMKI $\alpha$  (K54R and K49R, respectively). No significant changes in the phosphatase resistance of the kinases were observed between the WT and KD mutant (Figure 2E,F). Furthermore, we examined whether phospho-CaMKI is dephosphorylated in living cells. CaMKI was transiently transfected into 293T cells alone or in combination with CaMKP. The transfected cells were stimulated with ionomycin, and the phosphorylation level of CaMKI was analyzed by Western blotting using a phospho-CaMKI-specific antibody. As shown in panels G and H of Figure 2, the phosphorylation level of CaMKI $\alpha$ (WT) and KD mutants markedly increased after stimulation with ionomycin (Figure 2G, lanes 8 and 11). Conversely, under the same conditions, the phosphorylation was significantly attenuated when the cells were cotransfected with CaMKP and CaMKI $\alpha$  (Figure 2G, lanes 9 and 12). In contrast, CaMKI $\delta$  in the cells cotransfected with CaMKP and CaMKI $\delta$  was hardly dephosphorylated by CaMKP (Figure 2G, lanes 3 and 6). Next, we conducted phosphatase assays using other Ser/Thr phosphatases such as PPM1A, PPM1B, and PPM1D. As shown in Figure 3, CaMKI $\delta$  was also highly resistant to dephosphorylation by phosphatases other than CaMKP, whereas CaMKI $\alpha$  was significantly dephosphorylated under the same conditions. These data suggest that CaMKI $\delta$  is phosphatase-resistant.

**The N-Terminal Region around Subdomain III of CaMKI $\delta$  Is the Region Responsible for the Phosphatase Resistance.** In this study, we showed that CaMKI $\delta$  was hardly dephosphorylated by CaMKP compared with CaMKI $\alpha$ . When we compared the primary sequences of CaMKI $\delta$  and CaMKI $\alpha$ , we noticed that the C-terminal sequence of CaMKI $\delta$  was quite different from that of CaMKI $\alpha$  (Figure 4A). To identify the region responsible for the phosphatase resistance, we prepared various deletion mutants and chimeric proteins of CaMKI $\delta$  and CaMKI $\alpha$ : CaMKI $\delta$ (1–327), CaMKI $\alpha$ (1–322), CaMKI $\delta$ (1–327)/CaMKI $\alpha$ (323–374) ( $\delta/\alpha$ ), and CaMKI $\alpha$ (1–322)/CaMKI $\delta$ (328–433) ( $\alpha/\delta$ ), with His<sub>6</sub> tags on their C-termini (Figure 4B). To compare the phosphatase resistance among these mutants, we conducted *in vitro* phosphatase assays using CaMKP. As shown in Figure 4C–F, the phosphatase resistance of the deletion mutants and chimeric mutants of CaMKI $\delta$  and CaMKI $\alpha$  was the same as that of their wild-type counterparts. These results indicate that the C-terminal region of the CaMKI family enzymes (CaMKI $\alpha$ , residues 323–374; and CaMKI $\delta$ , residues 328–433) is not essential for the phosphatase resistance of CaMKI.

Next, to identify the region responsible for the phosphatase resistance, we prepared more chimeric mutants (chimeras 1–

3), which were fusion proteins of the N-terminal domain of CaMKI $\alpha$  and the C-terminal domain of CaMKI $\delta$  (Figure 5A). When we conducted the phosphatase assays using these chimera mutants, the chimera 1 mutant was hardly dephosphorylated by CaMKP, but chimera 2 and 3 mutants were significantly dephosphorylated under the same conditions (Figure 5B,C). The chimera 1 mutant contained subdomains III–XI of CaMKI $\delta$ , and the chimera 2 mutant contained subdomains VI–XI of CaMKI $\delta$ . These results suggest that subdomains III–V of CaMKI $\delta$  are responsible for the phosphatase resistance. Furthermore, we prepared additional chimeric mutants (chimeras 1-1, 1-2, and 1-3), which were fusion proteins of the N-terminal domain of CaMKI $\alpha$  and the C-terminal domain of CaMKI $\delta$  (Figure 5D). When we conducted the phosphatase assays using these chimeric mutants, they were significantly dephosphorylated as in the case of the chimera 2 mutant (Figure 5E,F). These results suggest that the N-terminal region around subdomain III of CaMKI $\delta$  plays an important role in phosphatase resistance.

In an attempt to identify the key sites responsible for the phosphatase resistance in CaMKI $\delta$ , we focused on the five amino acid residues, Pro-57, Lys-62, Ser-66, Ile-68, and Arg-76, located in subdomain III of CaMKI $\delta$ , as they were different between CaMKI $\delta$  and CaMKI $\alpha$  in various species (Figure 6A). To explore which residues in CaMKI $\delta$  are essential for phosphatase resistance, we prepared various point mutants of CaMKI $\delta$ : CaMKI $\delta$ (P57A), CaMKI $\delta$ (K62E), CaMKI $\delta$ (S66G), CaMKI $\delta$ (I68M), CaMKI $\delta$ (S66G,I68M:Double), and CaMKI $\delta$ (R76H). When we conducted the phosphatase assays using these mutants as substrates, CaMKI $\delta$ (R76H) was more readily dephosphorylated by CaMKP than the other point mutants (Figure 6B,C). Therefore, in the next experiment, we constructed various combination mutants of CaMKI $\delta$  containing the R76H mutation: CaMKI $\delta$ (P57A,R76H), CaMKI $\delta$ (K62E,R76H), and CaMKI $\delta$ (Double,R76H). In these mutants, CaMKI $\delta$ (Double,R76H) was more readily dephosphorylated by CaMKP than the other mutants (Figure 6D,E). Moreover, we constructed various combination mutants of CaMKI $\delta$ (Double,R76H): CaMKI $\delta$ (P57A,Double,R76H), CaMKI $\delta$ (K62E,Double,R76H), and CaMKI $\delta$ (S66G,Double,R76H). Surprisingly, although the “All” mutant was markedly dephosphorylated by CaMKP, CaMKI $\delta$ (P57A,Double,R76H) and CaMKI $\delta$ (K62E,Double,R76H) were less significantly dephosphorylated than the “All” mutant under the same conditions (Figure 6F,G). To examine whether this can be applied to other protein phosphatases, CaMKI $\delta$ (WT), CaMKI $\delta$ (All), and CaMKI $\alpha$ (WT) were dephosphorylated by PPM1A, PPM1B, and PPM1D. Figure 7 shows that CaMKI $\delta$ (All) was significantly dephosphorylated to an extent similar to that of CaMKI $\alpha$ (WT) by these phosphatases. These results strongly suggest that all five residues of CaMKI $\delta$ , Pro-57, Lys-62, Ser-66, Ile-68, and Arg-76, are critical for phosphatase resistance, irrespective of the protein phosphatases responsible for its dephosphorylation, though the contribution of each residue is unclear.

**The N-Terminal Region of CaMKI $\delta$  Is Essential for Its Phosphatase Resistance in Cells.** In this study, we revealed that the N-terminal region of CaMKI $\delta$  is important for its phosphatase resistance *in vitro*. Next, we examined whether like CaMKI $\alpha$ (WT), the CaMKI $\delta$  “All” mutant is significantly dephosphorylated by CaMKP in mammalian cells. CaMKI was transiently transfected into 293T cells alone or in combination with CaMKP. The transfected cells were

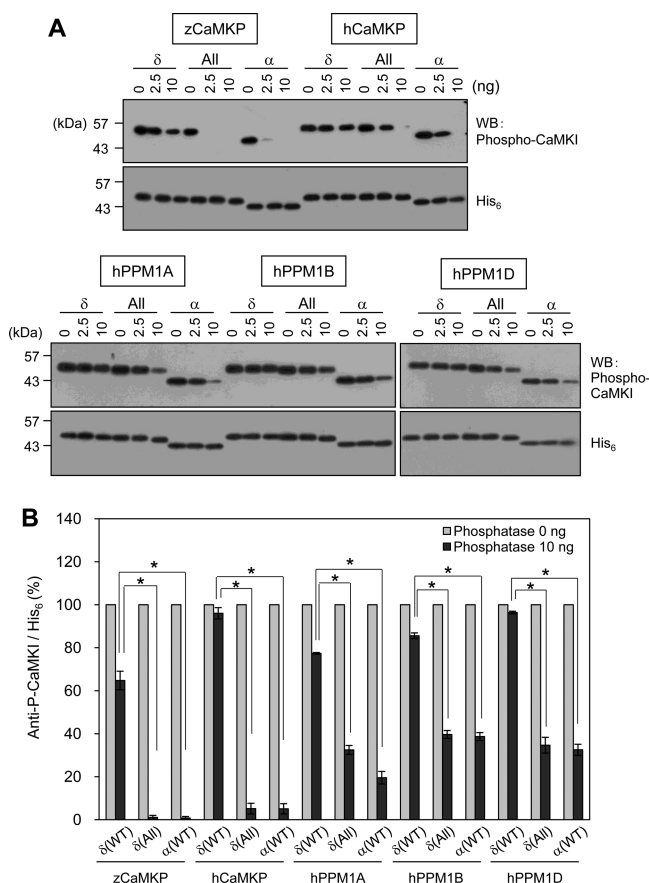


**Figure 7.** Dephosphorylation of the “All” mutant of CaMKI $\delta$  by other Ser/Thr phosphatases such as PPM1A, PPM1B, and PPM1D *in vitro*. (A) The indicated phosphatase activities were assessed using phosphorylated CaMKI $\alpha$ , CaMKI $\delta$ , or CaMKI $\delta$  “All” mutant as a substrate. Dephosphorylation of the CaMKIs was monitored by Western blotting with an anti-phospho-CaMKI antibody (top panel), and total CaMKI was detected by an anti-His<sub>6</sub> antibody (bottom panel). (B) Phospho-CaMKI (A, top panel) and total CaMKI (A, bottom panel) were quantified by Scion Image software and are indicated as phospho-CaMKI/total CaMKI. Data are means  $\pm$  SD of three independent determinations. Asterisks denote significant differences as determined by a Student’s *t* test ( $p < 0.005$ ).

stimulated with ionomycin, followed by Western blotting analysis using a phospho-CaMKI-specific antibody, to examine the phosphorylation level of CaMKI in the cells. As shown in Figure 8A, the phosphorylation level of CaMKI markedly increased when the CaMKI-transfected cells were treated with ionomycin (Figure 8A, lanes 2, 5, and 8). As expected, in contrast to wild-type CaMKI $\delta$ , the “All” mutant of CaMKI $\delta$  (P57A, K62E, S66G, I68M, R76H) was dephosphorylated by CaMKP (Figure 8A, lanes 3 and 6). The immunoreactive bands were quantitated using Scion Image software (Figure 8B). These results indicate that the phosphatase resistance of CaMKI $\delta$  is ascribed to the difference in the primary structure of its subdomain III compared with the primary structure of that of CaMKI $\alpha$ .

## DISCUSSION

In this study, we show that CaMKI $\delta$  has unusual phosphatase resistance, because of its unique structure in the N-terminal domain; thereby, it was anomalously phosphorylated and primed in 293T cells. The primed form of CaMKI $\delta$  was more

readily activated than other isoforms of CaMKI such as CaMKI $\alpha$ , leading to enhancement of CREB phosphorylation even at low Ca<sup>2+</sup> levels.

CaMKI has an autoinhibitory domain and a CaM-binding domain in the C-terminal region to regulate its kinase activity. In the presence of Ca<sup>2+</sup>, CaM binds to the CaM-binding domain of CaMKI to relieve the autoinhibition, which in turn results in phosphorylation by CaMKK of Thr-177 in the activation loop of CaMKI to fully activate it.<sup>6,7</sup> Therefore, in the resting state, cellular CaMKI should be in the inactive state, because of the low Ca<sup>2+</sup> levels in the cell. However, we found that Thr-182 (the equivalent of Thr-177 of rCaMKI $\alpha$ ) in the activation loop of CaMKI $\delta$  was highly phosphorylated even in the absence of stimulation that elevates the intracellular Ca<sup>2+</sup> level. Moreover, the constitutively phosphorylated CaMKI $\delta$  appeared to be active as evidenced by enhanced phosphorylation of the physiological CaMKI substrate, CREB, which was not observed with CaMKI $\alpha$  (Figure 1E,F). This observation led us to investigate the mechanism of the sustained phosphorylation and/or activation of CaMKI $\delta$  in the cells.

Ishikawa et al.<sup>38</sup> have reported that CaMKI $\delta$  was phosphorylated and/or activated in the resting state in HeLa cells, because of Ca<sup>2+</sup>-independent autonomous activity of CaMKK $\beta$ /3. It has also been reported that CaMKK $\alpha$  shows strictly Ca<sup>2+</sup>/CaM-dependent kinase activity, whereas CaMKK $\beta$  shows significant kinase activity even in the absence of Ca<sup>2+</sup>/CaM.<sup>39</sup> Therefore, we examined the *in vitro* phosphorylation of CaMKI $\delta$  and CaMKI $\alpha$  by CaMKK $\alpha$ . No significant difference in the phosphorylation time course was observed between them (Figure 2A,B). Similarly, no significant difference in the time course was observed between the CaMKK $\beta$ -catalyzed phosphorylation of CaMKI $\delta$  and CaMKI $\alpha$  (data not shown). Therefore, it is unlikely that CaMKI $\delta$  is more readily phosphorylated by CaMKK than CaMKI $\alpha$ , leading to the observed sustained phosphorylation of CaMKI $\delta$ .

Because CaMKI activity is supposed to be regulated not only by CaMKK but also by protein phosphatases responsible for dephosphorylation of Thr-177, we next examined the dephosphorylation of CaMKI $\delta$  and CaMKI $\alpha$  by CaMKP. Surprisingly, CaMKI $\delta$  was highly resistant to dephosphorylation by CaMKP, whereas CaMKI $\alpha$  was readily dephosphorylated by CaMKP. This was also the case with other Ser/Thr phosphatases such as PPM1A, PPM1B, and PPM1D, as CaMKI $\delta$  was also resistant to dephosphorylation by these phosphatases (Figures 3 and 7). On the basis of these lines of evidence, we concluded that the observed anomalous phosphorylation of CaMKI $\delta$  in the cells exists because of its resistance to dephosphorylation.

So far, little attention has been given to the regulation of CaMKI functions by dephosphorylation. Therefore, we conducted a detailed investigation of the dephosphorylation of CaMKI $\delta$  by CaMKP and found that the characteristic resistance of CaMKI $\delta$  to protein phosphatases can be ascribed to the structure of the N-terminal region of CaMKI $\delta$ . Using various CaMKI $\delta$  mutants, we clarified that only several amino acid residues located around subdomain III were critical for dephosphorylation of the Thr residue within the activation loop (Figures 5 and 6). In these experiments, however, we estimated the phosphatase resistance by changing the amounts of CaMKP and using a fixed concentration of the substrate, phospho-CaMKI $\delta$ , because of difficulties in performing detailed kinetic analysis. Therefore, we cannot exclude the possibility that CaMKI $\delta$  mutants in which we could not detect phosphatase

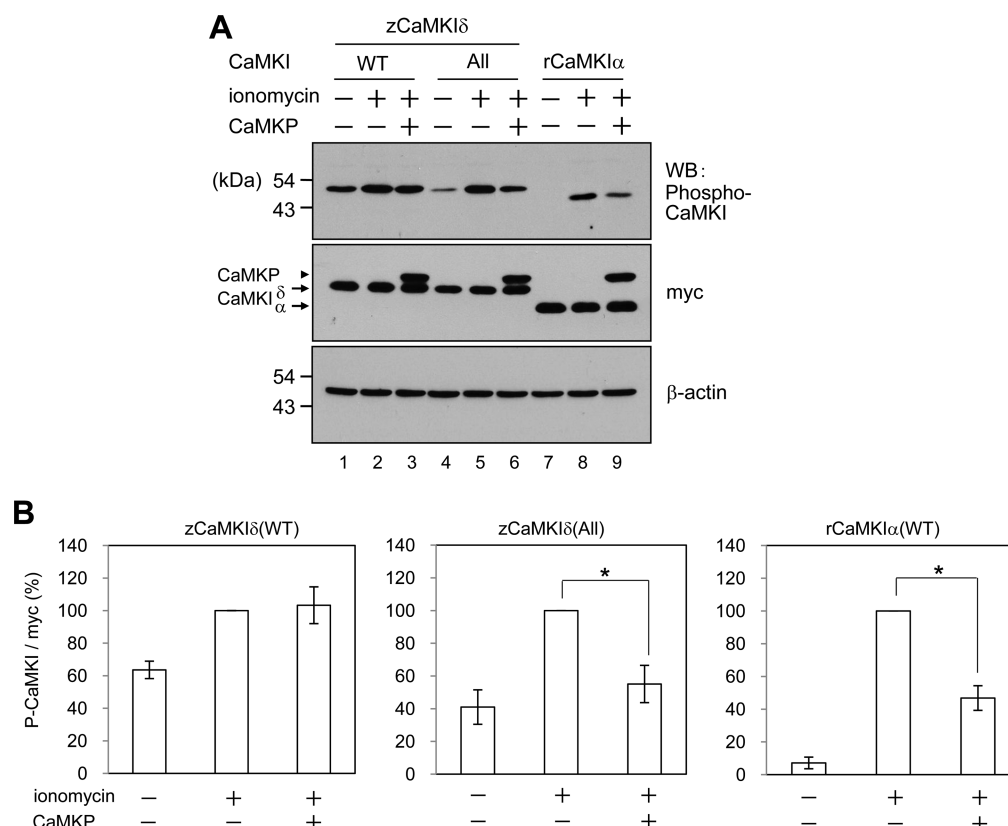


**Figure 8.** Dephosphorylation of the CaMKI $\delta$  "All" mutant by CaMKP in mammalian cells. (A) 293T cells transfected with pcDNA-CaMKIs alone or together with pcDNA-CaMKP were cultured for 24 h. Subsequently, the cells were cultured in serum-free medium for 6 h and stimulated with 1  $\mu$ M ionomycin for 5 min. The cells were lysed with SDS-PAGE sample buffer and analyzed by Western blotting with an anti-phospho-CaMKI antibody (top panel). The lysates were also analyzed by Western blotting using an anti-myc antibody to detect myc-tagged CaMKI (arrows) and myc-tagged CaMKP (arrowhead) (middle panel).  $\beta$ -Actin was examined by Western blotting with an anti- $\beta$ -actin antibody for loading control (bottom panel). (B) Phospho-CaMKI (A, top panel) and CaMKI (A, middle panel, arrows) were quantified by Scion Image software and are indicated as phospho-CaMKI/total CaMKI. The values are expressed as a percentage of the control (ionomycin +, CaMKP -). Data are means  $\pm$  SD of three independent determinations. Asterisks denote significant differences as determined by a Student's *t* test (*p* < 0.005).

resistance showed altered  $K_m$  values compared with those of wild-type CaMKI.

In subdomain III, there is an  $\alpha$ -helix called  $\alpha$ C, which is known to be important for ATP binding prior to conformational changes by phosphorylation of the Thr residue in the activation loop of various protein kinases.<sup>40–42</sup> In a proposed model of CaMKI $\alpha$ , the conformational change induced by ATP binding and CaM binding is supposed to be stabilized by ionic interactions between Glu-66 in  $\alpha$ C and Lys-49 within the ATP-binding region.<sup>42,43</sup> In CaMKI $\delta$ , however, several residues around Glu-66 in CaMKI $\alpha$  are replaced with other amino acids (Ala-57  $\rightarrow$  Pro, Glu-62  $\rightarrow$  Lys, and Met-68  $\rightarrow$  Ile). These replacements may induce a conformation of the  $\alpha$ C helix different from that of CaMKI $\alpha$ . Because the  $\alpha$ C helix is located near the activation loop in the tertiary structure of various protein kinases, it is possible that the difference in the conformation of the  $\alpha$ C helix affects the accessibility of the Thr residue to protein phosphatases, causing the characteristic phosphatase resistance of CaMKI $\delta$ .

Dephosphorylation of the Thr residue is likely to be independent of the kinase activity of CaMKI, because the kinase-dead mutants of CaMKI $\delta$  and CaMKI $\alpha$  (K54R and K49R, respectively) did not show altered kinetics of dephosphorylation of the Thr residue compared with those of the respective wild-type enzymes (Figure 2E–H). In this study, we found that as in the case of the zebrafish CaMKI $\delta$ , the

Thr residue in the activation loop of the mouse CaMKI $\delta$  was significantly phosphorylated by CaMKK without  $\text{Ca}^{2+}$  stimulation, suggesting that the observed phosphatase resistance of CaMKI $\delta$  is conserved among vertebrates. Once CaMKI $\delta$  is phosphorylated and/or activated by the upstream kinase CaMKK, it becomes resistant to protein phosphatases because of its unique structure in the N-terminal region. The constitutively phosphorylated CaMKI $\delta$  would be in a primed state, which can more readily be activated in response to  $\text{Ca}^{2+}$  signals than ordinary CaMKI such as CaMKI $\alpha$ , leading to an increased level of phosphorylation of CaMKI substrates such as CREB. This may contribute to acceleration or potentiation of  $\text{Ca}^{2+}$  signaling in a variety of vertebrate cells.

CREB is thought to be a physiological substrate of CaMKI.<sup>44</sup> It has been reported that CaMKI $\delta$  expressed in PC12 cells phosphorylates Ser-133 of CREB upon ionomycin stimulation, enhancing the transcriptional activity of CREB.<sup>26</sup> Phosphorylation of Ser-133 of CREB by CaMKI $\alpha$  and CaMKI $\gamma$  has also been reported to be involved in dendrite formation via upregulation of Wnt.<sup>22</sup> Furthermore, it has been reported that CaMKI $\alpha$ -catalyzed phosphorylation of CREB positively regulates neuroprotective signaling pathways induced by brain ischemia through activation of synaptic N-methyl-D-aspartate (NMDA) receptors and upregulation of brain-derived neurotrophic factor (BDNF).<sup>45</sup> Sakagami et al.<sup>26</sup> have shown that CaMKI $\delta$  expressed in hippocampal neurons was mostly



localized in the cytosol but rapidly translocated into the nucleus upon KCl stimulation. On the other hand, CaMKI $\alpha$  expressed in the neuron hardly altered its localization upon KCl stimulation. In our recent study,<sup>10</sup> we have found that the endogenous CaMKI $\delta$  in zebrafish fibroblasts was present in both the cytosol and the nucleus. Although the regulatory mechanism of the intracellular localization of CaMKI $\delta$  is currently unknown, it is likely that the priming of CaMKI $\delta$  by robust phosphorylation of Thr-182 is involved in the regulation of its localization. If this is the case, the endogenous CaMKI $\delta$  in zebrafish fibroblasts is probably, at least in part, in the primed state under low-Ca<sup>2+</sup> conditions.

Activation of CaMKI by an increase in the intracellular Ca<sup>2+</sup> level is involved in a variety of signal transduction pathways in the cell. Among CaMKI isoforms, both CaMKI $\alpha$  and CaMKI $\delta$  are cytosolic enzymes that show similar substrate specificity. The former is susceptible to protein phosphatases, whereas the latter is resistant to them. This suggests different physiological roles of CaMKI isoforms. Constitutive priming of CaMKI $\delta$  by resistance to protein phosphatases, reported here, may be a molecular mechanism for ensuring neuronal signaling by efficient phosphorylation of CaMKI substrate proteins, even under low-Ca<sup>2+</sup> conditions or with enhanced phosphatase activity.

## AUTHOR INFORMATION

### Corresponding Authors

\*Laboratory of Molecular Brain Science, Graduate School of Integrated Arts and Sciences, Hiroshima University, Higashi-Hiroshima 739-8521, Japan. Telephone: +81-82-424-6526. Fax: +81-82-424-0759. E-mail: aishida@hiroshima-u.ac.jp.

\*Department of Life Sciences, Faculty of Agriculture, Kagawa University, Ikenobe 2393, Miki-cho, Kagawa 761-0795, Japan. Telephone and fax: +81-87-891-3114. E-mail: sueyoshi@ag.kagawa-u.ac.jp.

### Funding

This work was supported in part by Grants-in Aid for Scientific Research from the Ministry of Education, Culture, Sports, Science and Technology of Japan, Research Fellowships of the Japan Society for the Promotion of Science for Young Scientists, an AIST research grant, and Kagawa University Specially Promoted Research Fund 2013.

### Notes

The authors declare no competing financial interest.

## ACKNOWLEDGMENTS

We thank Dr. Leslie Sargent Jones (Department of Biology, Appalachian State University, Boone, NC) for her helpful comments on the manuscript.

## ABBREVIATIONS

CaM, calmodulin; CaMKI, Ca<sup>2+</sup>/calmodulin-dependent protein kinase I; CaMKK, Ca<sup>2+</sup>/calmodulin-dependent protein kinase kinase; CaMKP, Ca<sup>2+</sup>/calmodulin-dependent protein kinase phosphatase; CREB, cyclic AMP-responsive element-binding protein; DMEM, Dulbecco's modified Eagle's medium; DTT, dithiothreitol; FCS, fetal calf serum; IPTG, isopropyl  $\beta$ -D-thiogalactopyranoside; SD, standard deviation.

## REFERENCES

- (1) Manning, G., Plowman, G. D., Hunter, T., and Sudarsanam, S. (2002) Evolution of protein kinase signaling from yeast to man. *Trends Biochem. Sci.* 27, 514–520.
- (2) Johnson, L. N., Noble, M. E., and Owen, D. J. (1996) Active and inactive protein kinases: Structural basis for regulation. *Cell* 85, 149–158.
- (3) Hardie, D. G. (1990) Roles of protein kinases and phosphatases in signal transduction. *Symp. Soc. Exp. Biol.* 44, 241–255.
- (4) Hook, S. S., and Means, A. R. (2001) Ca<sup>2+</sup>/CaM-dependent kinases: From activation to function. *Annu. Rev. Pharmacol. Toxicol.* 41, 471–505.
- (5) Ikeda, A., Okuno, S., and Fujisawa, H. (1991) Studies on the generation of Ca<sup>2+</sup>/calmodulin-independent activity of calmodulin-dependent protein kinase II by autophosphorylation. Autothiophosphorylation of the enzyme. *J. Biol. Chem.* 266, 11582–11588.
- (6) Haribabu, B., Hook, S. S., Selbert, M. A., Goldstein, E. G., Tomhave, E. D., Edelman, A. M., Snyderman, R., and Means, A. R. (1995) Human calcium-calmodulin dependent protein kinase I: cDNA cloning, domain structure and activation by phosphorylation at threonine-177 by calcium-calmodulin dependent protein kinase I kinase. *EMBO J.* 14, 3679–3686.
- (7) Tokumitsu, H., Enslen, H., and Soderling, T. R. (1995) Characterization of a Ca<sup>2+</sup>/calmodulin-dependent protein kinase cascade. Molecular cloning and expression of calcium/calmodulin-dependent protein kinase kinase. *J. Biol. Chem.* 270, 19320–19324.
- (8) Selbert, M. A., Anderson, K. A., Huang, Q. H., Goldstein, E. G., Means, A. R., and Edelman, A. M. (1995) Phosphorylation and activation of Ca<sup>2+</sup>-calmodulin-dependent protein kinase IV by Ca<sup>2+</sup>-calmodulin-dependent protein kinase Ia kinase. Phosphorylation of threonine 196 is essential for activation. *J. Biol. Chem.* 270, 17616–17621.
- (9) Senga, Y., Nagamine, T., Kameshita, I., and Sueyoshi, N. (2012) Knockdown of two splice variants of Ca<sup>2+</sup>/calmodulin-dependent protein kinase I $\delta$  causes developmental abnormalities in zebrafish, *Danio rerio*. *Arch. Biochem. Biophys.* 517, 71–82.
- (10) Senga, Y., Yoshioka, K., Kameshita, I., and Sueyoshi, N. (2013) Expression and gene knockdown of zebrafish Ca<sup>2+</sup>/calmodulin-dependent protein kinase I $\delta$ -LL. *Arch. Biochem. Biophys.* 540, 41–52.
- (11) Strack, S., Barban, M. A., Wadzinski, B. E., and Colbran, R. J. (1997) Differential inactivation of postsynaptic density-associated and soluble Ca<sup>2+</sup>/calmodulin-dependent protein kinase II by protein phosphatases 1 and 2A. *J. Neurochem.* 68, 2119–2128.
- (12) Lisman, J. E., and Zhabotinsky, A. M. (2001) A model of synaptic memory: A CaMKII/PP1 switch that potentiates transmission by organizing an AMPA receptor anchoring assembly. *Neuron* 31, 191–201.
- (13) Yoshimura, Y., Sogawa, Y., and Yamauchi, T. (1999) Protein phosphatase 1 is involved in the dissociation of Ca<sup>2+</sup>/calmodulin-dependent protein kinase II from postsynaptic densities. *FEBS Lett.* 446, 239–242.
- (14) Tokumitsu, H., Brickey, D. A., Glod, J., Hidaka, H., Sikela, J., and Soderling, T. R. (1994) Activation mechanisms for Ca<sup>2+</sup>/calmodulin-dependent protein kinase IV. Identification of a brain CaM-kinase IV kinase. *J. Biol. Chem.* 269, 28640–28647.
- (15) Park, I. K., and Soderling, T. R. (1995) Activation of Ca<sup>2+</sup>/calmodulin-dependent protein kinase (CaM-kinase) IV by CaM-kinase kinase in Jurkat T lymphocytes. *J. Biol. Chem.* 270, 30464–30469.
- (16) Kasahara, J., Fukunaga, K., and Miyamoto, E. (1999) Differential effects of a calcineurin inhibitor on glutamate-induced phosphorylation of Ca<sup>2+</sup>/calmodulin-dependent protein kinases in cultured rat hippocampal neurons. *J. Biol. Chem.* 274, 9061–9067.
- (17) DeRemer, M. F., Saeli, R. J., Brautigan, D. L., and Edelman, A. M. (1992) Ca<sup>2+</sup>-calmodulin-dependent protein kinases Ia and Ib from rat brain. II. Enzymatic characteristics and regulation of activities by phosphorylation and dephosphorylation. *J. Biol. Chem.* 267, 13466–13471.
- (18) Ishida, A., Okuno, S., Kitani, T., Kameshita, I., and Fujisawa, H. (1998) Regulation of multifunctional Ca<sup>2+</sup>/calmodulin-dependent

protein kinases by  $\text{Ca}^{2+}$ /calmodulin-dependent protein kinase phosphatase. *Biochem. Biophys. Res. Commun.* 253, 159–163.

(19) Onouchi, T., Sueyoshi, N., Ishida, A., and Kameshita, I. (2012) Phosphorylation and activation of nuclear  $\text{Ca}^{2+}$ /calmodulin-dependent protein kinase phosphatase (CaMKP-N/PPM1E) by  $\text{Ca}^{2+}$ /calmodulin-dependent protein kinase I (CaMKI). *Biochem. Biophys. Res. Commun.* 422, 703–709.

(20) Schmitt, J. M., Guire, E. S., Saneyoshi, T., and Soderling, T. R. (2005) Calmodulin-dependent kinase kinase/calmodulin kinase I activity gates extracellular-regulated kinase-dependent long-term potentiation. *J. Neurosci.* 25, 1281–1290.

(21) Guire, E. S., Oh, M. C., Soderling, T. R., and Derkach, V. A. (2008) Recruitment of calcium-permeable AMPA receptors during synaptic potentiation is regulated by CaM-kinase I. *J. Neurosci.* 28, 6000–6009.

(22) Wayman, G. A., Impey, S., Marks, D., Saneyoshi, T., Grant, W. F., Derkach, V., and Soderling, T. R. (2006) Activity-dependent dendritic arborization mediated by CaM-kinase I activation and enhanced CREB-dependent transcription of Wnt-2. *Neuron* 50, 897–909.

(23) Uboha, N. V., Flajolet, M., Nairn, A. C., and Picciotto, M. R. (2007) A calcium- and calmodulin-dependent kinase I $\alpha$ /microtubule affinity regulating kinase 2 signaling cascade mediates calcium-dependent neurite outgrowth. *J. Neurosci.* 27, 4413–4423.

(24) Saneyoshi, T., Wayman, G., Fortin, D., Davare, M., Hoshi, N., Nozaki, N., Natsume, T., and Soderling, T. R. (2008) Activity-dependent synaptogenesis: Regulation by a CaM-kinase kinase/CaM-kinase I/ $\beta$ PIX signaling complex. *Neuron* 57, 94–107.

(25) Davare, M. A., Fortin, D. A., Saneyoshi, T., Nygaard, S., Kaech, S., Banker, G., Soderling, T. R., and Wayman, G. A. (2009) Transient receptor potential canonical 5 channels activate  $\text{Ca}^{2+}$ /calmodulin kinase I $\gamma$  to promote axon formation in hippocampal neurons. *J. Neurosci.* 29, 9794–9808.

(26) Sakagami, H., Kamata, A., Nishimura, H., Kasahara, J., Owada, Y., Takeuchi, Y., Watanabe, M., Fukunaga, K., and Kondo, H. (2005) Prominent expression and activity-dependent nuclear translocation of  $\text{Ca}^{2+}$ /calmodulin-dependent protein kinase I $\delta$  in hippocampal neurons. *Eur. J. Neurosci.* 22, 2697–2707.

(27) Ishida, A., Kameshita, I., and Fujisawa, H. (1998) A novel protein phosphatase that dephosphorylates and regulates  $\text{Ca}^{2+}$ /calmodulin-dependent protein kinase II. *J. Biol. Chem.* 273, 1904–1910.

(28) Hayashi, N., Matsubara, M., Takasaki, A., Titani, K., and Taniguchi, H. (1998) An expression system of rat calmodulin using T7 phage promoter in *Escherichia coli*. *Protein Expression Purif.* 12, 25–28.

(29) Kinoshita, S., Sueyoshi, N., Shoji, H., Suetake, I., Nakamura, M., Tajima, S., and Kameshita, I. (2004) Cloning and characterization of a novel  $\text{Ca}^{2+}$ /calmodulin-dependent protein kinase I homologue in *Xenopus laevis*. *J. Biochem.* 135, 619–630.

(30) Sueyoshi, N., Takao, T., Nimura, T., Sugiyama, Y., Numano, T., Shigeri, Y., Taniguchi, T., Kameshita, I., and Ishida, A. (2007) Inhibitors of the  $\text{Ca}^{2+}$ /calmodulin-dependent protein kinase phosphatase family (CaMKP and CaMKP-N). *Biochem. Biophys. Res. Commun.* 363, 715–721.

(31) Kameshita, I., Tsuge, T., Kinashi, T., Kinoshita, S., Sueyoshi, N., Ishida, A., Taketani, S., Shigeri, Y., Tatsu, Y., Yumoto, N., and Okazaki, K. (2003) A new approach for the detection of multiple protein kinases using monoclonal antibodies directed to the highly conserved region of protein kinases. *Anal. Biochem.* 322, 215–224.

(32) Tada, Y., Nimura, T., Sueyoshi, N., Ishida, A., Shigeri, Y., and Kameshita, I. (2006) Mutational analysis of  $\text{Ca}^{2+}$ /calmodulin-dependent protein kinase phosphatase (CaMKP). *Arch. Biochem. Biophys.* 452, 174–185.

(33) Sueyoshi, N., Nimura, T., Ishida, A., Taniguchi, T., Yoshimura, Y., Ito, M., Shigeri, Y., and Kameshita, I. (2009)  $\text{Ca}^{2+}$ /calmodulin-dependent protein kinase phosphatase (CaMKP) is indispensable for normal embryogenesis in zebrafish, *Danio rerio*. *Arch. Biochem. Biophys.* 488, 48–59.

(34) Shimomura, S., Nagamine, T., Nimura, T., Sueyoshi, N., Shigeri, Y., and Kameshita, I. (2007) Expression, characterization, and gene knockdown of zebrafish doublecortin-like protein kinase. *Arch. Biochem. Biophys.* 463, 218–230.

(35) Sang, N., Condorelli, G., De Luca, A., MacLachlan, T. K., and Giordano, A. (1996) Generation of site-directed mutagenesis by extralong, high-fidelity polymerase chain reaction. *Anal. Biochem.* 233, 142–144.

(36) Laemmli, U. K. (1970) Cleavage of structural proteins during the assembly of the head of bacteriophage T4. *Nature* 227, 680–685.

(37) Bensadoun, A., and Weinstein, D. (1976) Assay of proteins in the presence of interfering materials. *Anal. Biochem.* 70, 241–250.

(38) Ishikawa, Y., Tokumitsu, H., Inuzuka, H., Murata-Hori, M., Hosoya, H., and Kobayashi, R. (2003) Identification and characterization of novel components of a  $\text{Ca}^{2+}$ /calmodulin-dependent protein kinase cascade in HeLa cells. *FEBS Lett.* 550, 57–63.

(39) Tokumitsu, H., Iwabu, M., Ishikawa, Y., and Kobayashi, R. (2001) Differential regulatory mechanism of  $\text{Ca}^{2+}$ /calmodulin-dependent protein kinase kinase isoforms. *Biochemistry* 40, 13925–13932.

(40) Yang, J., Cron, P., Good, V. M., Thompson, V., Hemmings, B. A., and Barford, D. (2002) Crystal structure of an activated Akt/protein kinase B ternary complex with GSK3-peptide and AMP-PNP. *Nat. Struct. Biol.* 9, 940–944.

(41) Huse, M., and Kuriyan, J. (2002) The conformational plasticity of protein kinases. *Cell* 109, 275–282.

(42) Zha, M., Zhong, C., Ou, Y., Han, L., Wang, J., and Ding, J. (2012) Crystal structures of human CaMKI $\alpha$  reveal insights into the regulation mechanism of CaMKI. *PLoS One* 7, e44828.

(43) Goldberg, J., Nairn, A. C., and Kuriyan, J. (1996) Structural basis for the autoinhibition of calcium/calmodulin-dependent protein kinase I. *Cell* 84, 875–887.

(44) Sheng, M., Thompson, M. A., and Greenberg, M. E. (1991) CREB: A  $\text{Ca}^{2+}$ -regulated transcription factor phosphorylated by calmodulin-dependent kinases. *Science* 252, 1427–1430.

(45) Sasaki, T., Takemori, H., Yagita, Y., Terasaki, Y., Uebi, T., Horike, N., Takagi, H., Susumu, T., Teraoka, H., Kusano, K., Hatano, O., Oyama, N., Sugiyama, Y., Sakoda, S., and Kitagawa, K. (2011) SIK2 is a key regulator for neuronal survival after ischemia via TORC1-CREB. *Neuron* 69, 106–119.